Proceedings of ALGORITMY 2012
pp. 200–208

MORTAR-LIKE MIXED-HYBRID METHODS FOR ELLIPTIC PROBLEMS ON COMPLEX GEOMETRIES. *

JAN BŘEZINA†

Abstract. We consider a model of the flow in fractured porous media based on the dual continuum approach and explicit description of the fracture zones by lower-dimensional objects. For this model, we present the mixed-hybrid formulation and discretization using Raviart-Thomas finite elements. In particular, we present two new methods for the discrete coupling between equations on meshes of different dimensions with arbitrary overlapping. Convergence properties of these methods are demonstrated by numerical tests.

Key words. fracture flow, mortar methods, mixed-hybrid finite elements

1. Introduction. Realistic modeling of subsurface water flow has to deal with highly heterogeneous and multi-scale nature of the hydraulic properties of the rock masses. The water moves slowly on the majority of the rock volume through microscopic pores and fractures while it moves rapidly on the small part of the rock volume occupied by larger fractures that forms preferential flow paths. These paths may by highly localized and the volumetric flow rate in them may be comparable or even dominating flow rate in the bulk volume. However, a cross-section of the larger fractures is still very small compared to the length scale of the whole domain, thus one has to refine computational mesh along the fractures in order to render them properly, which can lead to the meshes that are intractably larger, especially if the network of fractures is dense enough. To overcome these difficulties, we consider the flow on fractures to be constant in the normal direction and we integrate the flow equations over the aperture of the fractures. Similar procedure can be done for the channels with relatively small cross-section area. Finally, we obtain system of equations on the domains of different dimension, coupled through the boundary conditions. This approach has been proposed by several authors, see e.g. [5] or homogenization arguments in [4].

Even after this simplification, it could be difficult to obtain the mesh where the elements on the fractures match the sides of the elements of a surrounding continuum. The aim of this paper is to present two mortar-like methods for mixed-hybrid formulation that relax this compatibility condition. Since these methods can not capture the jump in the pressure over the fractures, we have to assume continuous pressure in our model. This is not completely unrealistic, since such a model can be viewed as a dual continuum model in spirit of Gerke and Genuchten [3] where the fracture zone is explicitly localized.

The paper is organized as follows. In the next section, we specify our model. Then, in Section 3, we introduce its mixed-hybrid formulation. The two new methods for discretization on incompatible meshes are presented in Section 4 and the last section is devoted to the numerical test of convergence of the methods.

*This work was supported by the Technology Agency of the Czech Republic under the project no. TA01021331.

†Technical University in Liberec, Studentská 2, Liberec, Czech Republic (jan.brezina@tul.cz).

2. Problem formulation. Let Ω_3 be a domain in $\mathbf{R}^3$, $\Omega_2 \subset \mathbf{R}^3$ a domain of fractures formed by piecewise smooth manifolds, and $\Omega_1 \subset \mathbf{R}^3$ a domain of channels formed by piecewise smooth curves. In order to keep further formulas consistent, we also introduce Ω_0 as the set of channel intersections. We assume that Ω_1 has no direct interaction with Ω_3, i.e.

$$\Omega_1 \cap \Omega_3 \subset \Omega_2. \tag{2.1}$$

We also assume that the boundary of Ω_d is outside of Ω_{d+1} for $d = 1, 2$. On the other hand, the domain Ω_d can hang out of Ω_{d+1} for $d = 1, 2$.

On these domains, we consider the Darcy's law

$$\boldsymbol{q}_d = \nu_d \boldsymbol{v}_d = -\nu_d \mathbb{K}_d \nabla h_d \quad \text{on } \Omega_d \setminus \Omega_{d-1} \quad \text{for } d = 1, 2, 3; \tag{2.2}$$

and the continuity equation

$$\mathrm{div} \boldsymbol{q}_d = F_d \quad \text{on } \Omega_d \setminus \Omega_{d-1} \quad \text{for } d = 1, 2, 3; \tag{2.3}$$

where $\boldsymbol{v}_d$ $[ms^{-1}]$ is the velocity $\boldsymbol{q}_d$ is the Darcy flux and ν_d is the measure of cross-section. The physical units of these quantities depends on the dimension

$\boldsymbol{q}_3$ $[ms^{-1}]$,	ν_3 $[-]$	is constantly one,
$\boldsymbol{q}_2$ $[m^2 s^{-1}]$,	ν_2 $[m]$	is fracture's aperture,
$\boldsymbol{q}_1$ $[m^3 s^{-1}]$,	ν_1 $[m^2]$	is channel's cross-section area.

Other quantities in (2.2) and (2.3) are: the tensor of hydraulic conductivity $\mathbb{K}_d$, the pressure head h_d $[m]$, and partially integrated density of the water sources F_d. Vectors $\boldsymbol{q}_d$ and tensors $\mathbb{K}_d$ lives in the corresponding local tangent spaces of domains Ω_d. The principal unknowns of this system are the fluxes $\boldsymbol{q}_d$ and the pressure heads h_d.

To complete the system, we have to prescribe boundary conditions. The boundary of $\Omega_d \setminus \Omega_{d-1}$ consists of the outer boundary $\partial\Omega_d$ and the interior interface to the domain Ω_{d-1}. On the outer boundary, we consider the Dirichlet boundary condition $h_d = H_d$ on the set Γ_d^D and the homogeneous Neumann boundary condition on the set Γ_d^N, where these two sets forms disjoint decomposition of $\partial\Omega_d$. The boundary conditions on the interior interfaces introduce a coupling between dimensions. For $d = 3$, the set $\Omega_2 \cap \Omega_3 \setminus \Omega_1$ consists of separated patches of smooth two side manifolds, thus we need two boundary conditions on them. First condition is the continuity of h_3 on both sides of the patch and the second is balance of the fluxes

$$\boldsymbol{q}_3^+ \cdot \boldsymbol{n}^+ + \boldsymbol{q}_3^- \cdot \boldsymbol{n}^- = Q_3 = \sigma_2(\mathrm{Tr}\, h_3 - h_2). \tag{2.4}$$

Here Q_3 is the surface density of the local outer flux from Ω_3 into Ω_2 which is proportional to the difference between the trace of h_3 and h_2 with a given transition coefficient σ_2 $[s^{-1}]$. The flux Q_3 also appears as a part of the volume source $F_2 = Q_3 + \nu_2 f_2$ on the domain Ω_2. For $d = 2$, the set $\Omega_1 \cap \Omega_2 \setminus \Omega_0$ consists of separated curve segments, where every segment is on the boundary of $k \geq 2$ different 2d-patches. The continuity of the pressure h_2 yields $k - 1$ conditions and the last condition is again balance of the fluxes

$$\sum_{i=1}^{k} \boldsymbol{q}_2^i \cdot \boldsymbol{n}^i = Q_2 = \sigma_1(\mathrm{Tr}\, h_2 - h_1). \tag{2.5}$$

Here $\sigma_1 = \nu_2\tilde{\sigma}_1$, where $\tilde{\sigma}_1$ $[s^{-1}]$ is the transition coefficient, and as before the flux Q_2 is a part of the volume source on Ω_1, i.e. $F_1 = Q_2 + \nu_1 f_1$. Similarly, we assume continuity of the pressure head h_1 and zero flux balance on the set Ω_0 and for the consistency, we introduce $Q_1 = 0$. Finally, we set $F_3 = f_3$, where f_d $[s^{-1}]$ is the density of external volume sources. For the sake of simplicity, we consider equations (2.4) and (2.5) also on hanging parts, namely on $\Omega_2 \setminus \Omega_1$ and $\Omega_1 \setminus \Omega_0$ respectively, but we set $\sigma_d = 0$ on $\Omega_d \setminus \Omega_{d+1}$ for $d = 1, 2$.

3. Mixed-Hybrid Formulation. After introduction of the model, we are going to derive its mixed-hybrid weak formulation in the similar fashion as in [1] and [7]. To avoid technicalities, we assume that Ω_3 have piecewise polygonal boundary, domain Ω_2 consists of polygons, and Ω_1 consists of line segments. We also assume that the Dirichlet boundary Γ_3^D is a polygonal subset of $\partial\Omega_3$. Further, we decompose Ω_d, $d = 1, 2, 3$, into sub-domains Ω_d^i, $i \in \mathcal{I}_d$, and we denote the set of their boundaries

$$\Gamma_d = \bigcup_{i\in\mathcal{I}_d} \partial\Omega_d^i.$$

For now, we consider only the decompositions satisfying the compatibility condition

$$\Omega_{d-1} \cap \Omega_d \subset \Gamma_d, \quad d = 1, 2, 3, \tag{3.1}$$

but we shall relax this condition on the discrete level.

In the following, we introduce spaces for the solution and the test functions. The fluxes $\boldsymbol{q}_d^i$ on the sub-domains Ω_d^i shall be from

$$V = V_3 \times V_2 \times V_1 = \prod_{d=3,2,1} \prod_{i\in\mathcal{I}_d} H(\mathrm{div}, \Omega_d^i), \tag{3.2}$$

where $H(\mathrm{div}, \Omega_d^i) \subset L^2(\Omega_d^i)^d$ is the standard space of vector functions with divergence in $L^2(\Omega_d^i)$. The pressure head h_d shall be from the space

$$P_d = L^2(\Omega_d), \tag{3.3}$$

and the trace of the pressure head $\mathring{h}_d$ from the space

$$\mathring{P}_d = \left\{ \mathring{\varphi} \in H^{\frac{1}{2}}(\Gamma_d) \,|\, \mathring{\varphi} = 0 \text{ on } \Gamma_d^D \right\}, \tag{3.4}$$

where $H^{\frac{1}{2}}(\partial\Omega)$ is the space of traces of functions from $H^1(\Omega)$. Equivalently, it can be introduced as the subspace of functions form $L^2(\Omega)$ with a finite norm

$$\|u\|^2_{H^{\frac{1}{2}}(\Omega)} = \int_\Omega u^2(x)\,\mathrm{d}x + \int_\Omega \int_\Omega \frac{|u(x) - u(y)|^2}{|x - y|^{d+1}}\,\mathrm{d}x\,\mathrm{d}y. \tag{3.5}$$

In particular, $\mathring{P}_1$ is just finite-dimensional vector space. We also introduce common space for the pressure head unknowns

$$P = P_3 \times P_2 \times P_1 \times \mathring{P}_3 \times \mathring{P}_2 \times \mathring{P}_1. \tag{3.6}$$

In order to derive the mixed-hybrid formulation, we divide (2.2) by $\nu_d\mathbb{K}_d$, multiply it by a vector test function $\boldsymbol{\psi}_d \in V_d$, and integrate by parts over every sub-domain Ω_d^i.

There appears a boundary term containing the trace of the pressure head $\mathring{h}_d$ which is further treated as an independent unknown. It can also be viewed as the Lagrange multiplier for the balance constrain

$$\sum_{i\in\mathcal{I}_d} \boldsymbol{q}_d\cdot\boldsymbol{n}|_{\partial\Omega_d^i} = \begin{cases} Q_d & \text{on } \Omega_{d-1}\cap\Gamma_d,\\ 0 & \text{on } \Gamma_d\setminus\Omega_{d-1},\end{cases} \tag{3.7}$$

imposed on the fluxes by (2.4), (2.5) and their continuity out of Ω_{d-1}. Next, we substitute for F_d in the continuity equation (2.3) and test it by $-\varphi_d\in P_d$. Finally, we substitute for Q_d in the balance constrain (3.7) and test this equation by the functions $\mathring{\varphi}_d\in\mathring{P}_d$ with support on $\Gamma_d\setminus\Gamma_d^D$. After these manipulations, we arrive at following definition of the mixed-hybrid solution in terms of an abstract saddle point problem:

DEFINITION 3.1. *We say that pair* $(\boldsymbol{q},\overline{h}) = \big(\boldsymbol{q},(h,\mathring{h})\big)\in V\times P$ *is mixed-hybrid solution of the problem* P_{123} *if it satisfies abstract saddle point problem*

$$a(\boldsymbol{q},\boldsymbol{\psi}) + b(\boldsymbol{\psi},\overline{h}) = \langle G,\boldsymbol{\psi}\rangle \qquad \forall\,\boldsymbol{\psi}\in V, \tag{3.8}$$

$$b(\boldsymbol{q},\overline{\varphi}) - c(\overline{h},\overline{\varphi}) = \langle F,\overline{\varphi}\rangle \qquad \forall\,\overline{\varphi}=(\varphi,\mathring{\varphi})\in P, \tag{3.9}$$

where the bilinear forms on the left-hand side are

$$a(\boldsymbol{q},\boldsymbol{\psi}) = \sum_{d=1,2,3}\sum_{i\in\mathcal{I}_d}\int_{\Omega_d^i}\frac{1}{\nu_d}\boldsymbol{q}_d^i\mathbb{K}_d^{-1}\boldsymbol{\psi}_d^i,$$

$$b(\boldsymbol{q},\overline{\varphi}) = \sum_{d=1,2,3}\sum_{i\in\mathcal{I}_d}\left(\int_{\Omega_d^i}-\mathrm{div}\boldsymbol{q}_d^i\,\varphi_d + \int_{\partial\Omega_d^i}(\boldsymbol{q}_d^i\cdot\boldsymbol{n})\mathring{\varphi}_d\right),$$

$$c(\overline{h},\overline{\varphi}) = \sum_{d=1,2}\int_{\Omega_d}\sigma_d(h_d-\mathring{h}_{d+1})(\varphi_d-\mathring{\varphi}_{d+1})$$

and linear forms on the right-hand side are

$$\langle G,\boldsymbol{\psi}\rangle = \sum_{d=1,2,3}\sum_{i\in\mathcal{I}_d}\int_{\partial\Omega_d^i}\tilde{H}_d(\boldsymbol{\psi}_d\cdot\boldsymbol{n}),$$

$$\langle F,\overline{\varphi}\rangle = -\sum_{d=1,2,3}\int_{\Omega_d}\nu_d f_d\varphi_d.$$

where $\tilde{H}_d$ *is an extension of the prescribed boundary pressure head* $H_d\in H^{1/2}(\Gamma_d^D)$ *into the space* $\mathring{P}_d$. *Consequently the full trace of the unknown pressure head is* $\mathring{h}_d+\tilde{H}_d$.

The second term in the bilinear form $b(\cdot,\cdot)$ deserves a note. The outflow $\boldsymbol{q}_d^i\cdot\boldsymbol{n}$ is from the dual of $H^{\frac{1}{2}}(\partial\Omega_d^i)$, therefore we have to use restriction of $\mathring{\varphi}_d$ from the space $H^{\frac{1}{2}}(\Gamma_d)$, where $\Omega_d^i\subsetneq\Gamma_d$. Fortunately, this restriction exists due to Gagliardo definition of $H^{\frac{1}{2}}$ spaces by the norm (3.5). In the bilinear form $c(\cdot,\cdot)$, we simply use embedding of $H^{\frac{1}{2}}(\Gamma_d)$ into $L^2(\Gamma_d)$.

Assuming that ν_d, $\mathbb{K}_d$, σ_d, and α_d are uniformly bounded and uniformly grater than zero (positive definiteness of $\mathbb{K}_d$), we can prove that $a(\cdot,\cdot)$ and $c(\cdot,\cdot)$ are bounded, symmetric, positive definite bilinear forms and that

$$\mathcal{B}: V\to P',\quad \langle\mathcal{B}(\boldsymbol{q},\varphi\rangle = b(\boldsymbol{q},\varphi)$$

is surjective operator. Assuming further

$$f_d \in L^2(\Omega_d) \quad \text{and} \quad H_d \in H^{\frac{1}{2}}(\Gamma_d^D),$$

we can prove that the mixed-hybrid solution is independent of choice of decomposition $\mathcal{I}_d$ and independent of choice of extension $\tilde{H}_d$. Finally, using [2, Theorem 1.2], we can prove existence and uniqueness of the mixed-hybrid solution.

4. Discretization on incompatible meshes. Let us consider particular decomposition of domains Ω_d into a mesh of simplex elements Ω_d^i, $i \in \mathcal{I}_d$. We say that the mesh is *compatible* if it satisfies condition (3.1) and if the elements of dimension $d-1$ match the faces of elements of dimension d. Otherwise we say that the mesh is *incompatible*. In this section, we shall deal with a discrete version of the mixed-hybrid problem 3.1 on the incompatible meshes.

First, let us consider discretization of 3.1 on the compatible mesh. We approximate the velocity space V by

$$\tilde{V} = \tilde{V}_3 \times \tilde{V}_2 \times \tilde{V}_1, \quad \tilde{V}_d = \prod_{i \in \mathcal{I}_d} \mathcal{RT}_0(\Omega_d^i), \tag{4.1}$$

where $\mathcal{RT}_0(\Omega_d^i)$ is $d+1$ dimensional space of Raviart-Thomas functions on one element (see [2]). The space P will be approximated by zero order polynomials. We approximate P_d by the polynomials constant over individual elements

$$\tilde{P}_d = \prod_{i \in \mathcal{I}_d} \mathcal{P}_0(\Omega_d^i), \tag{4.2}$$

and similarly, we approximate the space $\mathring{P}$ by the polynomials constant over the sides of elements

$$\tilde{P}_d^\circ = \prod_{e \in \mathcal{E}_d} \mathcal{P}_0(e), \tag{4.3}$$

where $\mathcal{E}_d$ is set of all edges on sides of the elements Ω_d^i, $i \in \mathcal{I}_d$ that are not on the Dirichlet boundary Γ_d^D. Note, that unlike the previous spaces, the space $\tilde{P}_d^\circ$ is not subspace of $\mathring{P}_d$, so the approximation is nonconforming. Finally, let us denote $\overline{P}_d = \tilde{P}_d \times \tilde{P}_d^\circ$ and $\tilde{P} = \overline{P}_3 \times \overline{P}_2 \times \overline{P}1$.

Using these spaces, we obtain a discrete linear system

$$\mathbb{A}\boldsymbol{x} = \boldsymbol{b}. \tag{4.4}$$

The values of the system matrix $\mathbb{A}$ are given directly by the bilinear forms a, b, c

$$A_{ij} = a(\boldsymbol{\psi}_j, \boldsymbol{\psi}_i) + b(\boldsymbol{\psi}_i, \overline{\varphi}_j) + b(\boldsymbol{\psi}_j, \overline{\varphi}_i) + c(\overline{\varphi}_j, \overline{\varphi}_i)$$

and the values of the right-hand side $\boldsymbol{b}$ are given by the linear forms F, G

$$b_i = \langle G, \boldsymbol{\psi}_i \rangle + \langle F, \overline{\varphi}_i \rangle,$$

where the bases functions $(\boldsymbol{\psi}_i, \overline{\varphi}_i)$ iterates through a suitable basis of $\tilde{V} \times \tilde{P}$. All integrals are evaluated as a sum of integrals over individual elements and their boundaries, in particular the term c is sum of the integrals over elements Ω_d^i for $d = 1, 2$

$$c(\overline{\varphi}_j, \overline{\varphi}_i) = \sum_{\substack{d=1,2 \\ k \in I_d}} \int_{\Omega_d^k} \sigma_d^k (\varphi_{d,j} - \mathring{\varphi}_{d+1,j})(\varphi_{d,i} - \mathring{\varphi}_{d+1,i}) \tag{4.5}$$

In order to get a discrete mixed-hybrid formulation on an incompatible mesh, we have to modify the bilinear form c. In particular we have to provide an approximation of the trace of the pressure head h_{d+1} on Ω_d since for meshes violating (3.1) this set is not in the support of $\mathring{h}_{d+1}$. We shall consider following approximation of c:

$$\tilde{c}(\overline{\varphi}_j, \overline{\varphi}_i) = \sum_{\substack{d=1,2 \\ k \in I_d}} \int_{\Omega_d^k} \sigma_d^k \big(S_d(\overline{\varphi}_{d,j}) - T_d(\overline{\varphi}_{d+1,j})\big)\big(S_d(\overline{\varphi}_{d,i}) - T_d(\overline{\varphi}_{d+1,i})\big), \tag{4.6}$$

where $S_d : \overline{P}_d \to L^2(\Omega_d)$ is a *reconstruction* operator, which can possibly reconstruct better approximation of h_d from its discrete version $\overline{h}_d$, and $T_d : \overline{P}_{d+1} \to L^2(\Omega_d)$ is approximation of the trace.

A straightforward choice for these operators is

$$S_d(\overline{\varphi}_d) = \varphi_d \quad \text{and} \quad T(\overline{\varphi}_{d+1})|_{\Omega_d^i \cap \Omega_{d+1}^j} = \varphi_{d+1}|_{\Omega_{d+1}^j}, \tag{4.7}$$

i.e. the approximation of the trace is possibly different constant on every intersection $\Omega_d^i \cap \Omega_{d+1}^j$. This choice was suggested by O. Severýn in [6], but it come out that for large values of σ the term $\tilde{c}$ force equivalence of the pressures h_d and h_{d+1} on all elements intersection the domain Ω_d which leads to wrong solution that is locally constant along Ω_d.

Thus we have proposed two other choices of operators S_d, T_d inspirited by the mortar methods.

4.1. method P0. In the first method, we take space P_d as a space of the mortar interface and let both S_d and T_d interpolate into this space. Thus, we take $S_d(\overline{\varphi}_d) = \varphi_d$ as before and

$$T(\overline{\varphi}_{d+1})|_{\Omega_d^i} = \frac{\sum_{j \in I_{d+1}} \mu_d^{ij} \varphi_{d+1}|_{\Omega_{d+1}^j}}{\sum_{j \in I_{d+1}} \mu_d^{ij}}, \tag{4.8}$$

i.e. T_d on Ω_d^i is a weighted average of the values on intersecting elements Ω_{d+1}^j with the weights proportional to the d-dimensional measure μ_d^{ij} of the intersection $\Omega_d^i \cap \Omega_{d+1}^j$. Clearly the sums in (4.8) run only over elements intersecting with Ω_d^i.

4.2. method P1. For the second method, we have to introduce a space of nonconforming finite elements $X_d \subset L^2(\Omega_d)$ of the functions φ that are linear on every element Ω_d^i and continuous in the midpoints of all edges from $\mathcal{E}_d$. In particular X_1 is the space of continuous piecewise linear functions. Since both $\tilde{P}^\circ$ and X_d has support points of degrees of freedom in the midpoints of edges, we can introduce operator $R : \tilde{P}^\circ \to X_d$ that reconstructs linear nonconforming approximation from the trace values on the edges given by $\mathring{\varphi}_d$. Then we set

$$S_d(\overline{\varphi}_d) = R(\mathring{\varphi}_d), \quad T_d(\overline{\varphi}_d)|_{\Omega_d^i \cap \Omega_{d+1}^j} = \mathrm{Tr}_{\Omega_d^i} R(\mathring{\varphi}_{d+1}). \tag{4.9}$$

Thus, on every intersection $\Omega_d^i \cap \Omega_{d+1}^j$ the value of T_d is a linear function that is the trace of $R(\mathring{\varphi}_{d+1})$.

Motivation for this method comes from the structure of the linear system (4.4). For compatible discretization, this system is indefinite, but by means of Schur complements, it can be efficiently reduced to a positive definite system only for traces of the pressure head. Method P1 does not break the structure of the system, thus the reduction of the system can be done in the same way.

5. Numerical experiments. In this section, we shall present numerical tests of convergence for the proposed methods P0 and P1. We present only tests for the case 2d-1d for the simple reason, that the case 3d-2d requires much more complicated algorithms from the computation geometry for identification of intersections $\Omega_d^i \cap \Omega_{d+1}^j$ and we do not have them implemented yet.

Let us consider a 2d-1d flow problem on the domains $\Omega_2 = (-1,1) \times (-1,1)$ and $\Omega_1 = \{(x,0) \,|\, x \in (-1,1)\}$. We set hydraulic conductivities $k_2 = 1$ and $k_1 = 5$ on Ω_2 and Ω_1 respectively, and we assume zero sources $f_1 = f_2 = 0$. We also set $\delta_1 = \delta_2 = 1$, which implies $\boldsymbol{q}_d = \boldsymbol{v}_d$, for $d = 1, 2$.

We prescribe the Dirichlet boundary condition $H_2 = 10$ on the top and the bottom part of $\partial\Omega_2$ and the homogeneous Neumann boundary conditions on the side edges. At the end points of Ω_1, we prescribe the Dirichlet boundary condition $H_1 = 5$. In our study, we consider three values for the parameter $\sigma = 1, 10, 100$; where the largest value force the pressures h_1 and h_2 to be close to the equilibrium while the smallest value let h_2 to be almost constant over Ω_2.

The setting just described admits an analytical solution in a form of Fourier series, which can be used as the reference solution $(h_d, \boldsymbol{q}_d)$, $d = 1, 2$. For computation of the numerical solution $(\tilde{h}_d, \tilde{\boldsymbol{q}}_d)$, $d = 1, 2$, we have used incompatible unstructured regular meshes with diameter of triangles in Ω_2 proportional to $\delta_2 = 2^{-k}$ and elements in Ω_1 proportional to $\delta_1 = \delta_2/\rho$. We have performed calculations for $k = 2, \ldots, 8$ and $\rho = 0.5, 1, 2$. To approximate the errors

$$\eta(h_d) = \left\|\tilde{h}_d - h_d\right\|_{L^2(\Omega_d)}, \quad \text{and} \quad \eta(\boldsymbol{q}_d) = \left\|\tilde{\boldsymbol{q}}_d - \boldsymbol{q}_d\right\|_{L^2(\Omega_d)}, d = 1, 2$$

we have used the midpoint rule on every element. Since we can expect at most quadratic convergence order for $\mathcal{RT}_0$ finite elements (see [8]), the midpoint rule should provide sufficient precision.

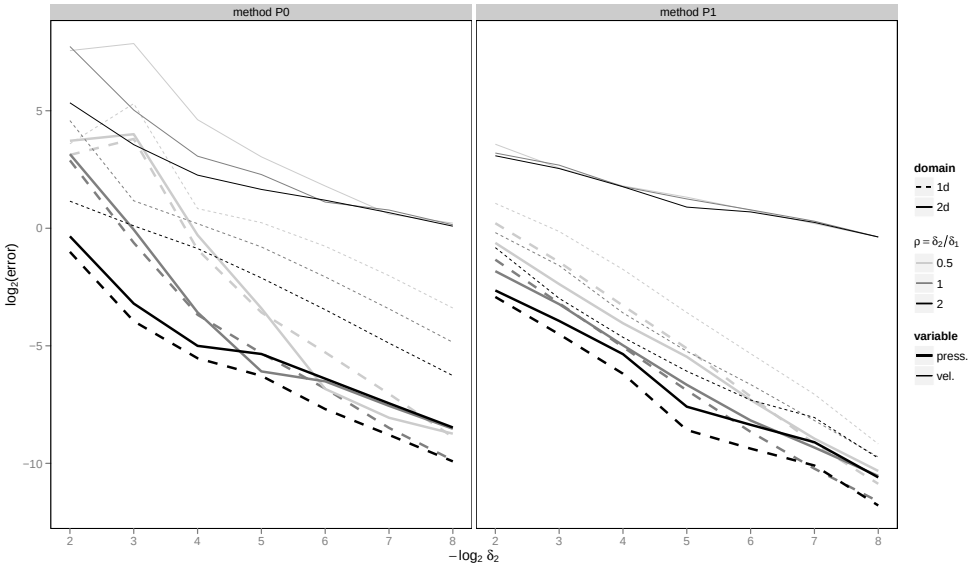

FIG. 5.1. *Approximative L^2-norm of the error for the pressure head and the velocity on both domains and for both methods with $\sigma = 100$.*

Before we proceed to the analysis of the order of convergence, we should discus the role of the parameter ρ. It is known from the theory of mortar methods that discretization of the mortar interface (fracture in our case) should not be finer then discretization of the surrounding sub-domains (see [9, Assumption 2.1]). This condition is not very restrictive in practice, however we can demonstrate it in Figure 5.1 that displays errors for the most sensitive case $\sigma = 100$. All black lines, which corresponds to $\rho = 2$, have smaller slope at the right hand part of plot that corresponds to the fine meshes. It means that the order of convergence is slightly deteriorated for large values of ρ in particular for the method P0 and for the error of h_1. On the other hand, for smaller values of ρ, the method P0 exhibits quite large errors on coarse meshes. This is caused by bad conditioning of the linear system. In fact for $\rho = 0.2$ (not on the plot), we get completely wrong solution on coarse meshes. The conclusion is that the method P0, unlike the method P1, requires δ_1 to be close to δ_2.

TABLE 5.1
Estimated order of convergence of approximated L^2-error for the pressure head and the velocity.

	pressure head				velocity			
	$\rho = 0.5$		$\rho = 1$		$\rho = 0.5$		$\rho = 1$	
	1d	2d	1d	2d	1d	2d	1d	2d
method P0	2.1	1.60	1.87	1.55	1.82	0.6	1.43	0.56
method P1	2.1	1.68	1.87	1.55	1.82	0.6	1.60	0.56
compatible mesh	1.9	1.9	1.9	1.9	1.9	1	1.9	1

For estimation of the order of convergence, we have used linear regression and analysis of variance to determine factors that influence the order of convergence. The results are summarized in Table 5.1. On the last line, there are also results for the convergence of solution on a compatible mesh. The values for both methods were very close and different values are reported only when the difference was statistically significant. Surprisingly the ratio ρ has stronger impact then the choice of the method. Value of the parameter σ has no significant influence on the order of convergence. On the other hand, the absolute magnitude of all errors save the error $\eta(\boldsymbol{v}_2)$ was two times larger for the method P0 then for the method P1.

Comparing to the compatible case, which exhibits almost optimal orders of convergence, the substantial difference is namely for $\eta(h_2)$ (about 3/2 for our method) and for $\eta(\boldsymbol{v}_2)$. Indeed, the order of convergence of the error $\eta(\boldsymbol{v}_2)$ should be about 1/2 since we have constant error ε on all elements along Ω_1 due to the bad resolution of the jump in the velocity, then

$$\eta(\boldsymbol{v}_2) > \sqrt{1/\delta_2 \varepsilon^2 \delta_2^2} = \varepsilon \sqrt{\delta_2}.$$

The last thing, we want to mention is conditioning of the discrete system. As was already mentioned, the system resulting from the discretization is indefinite, but one can apply Schur complements to obtain a reduced positive definite system. We have used CG solver to solve this system and as the side effect we have obtained approximative eigenvalues, which allows us to compute estimate of the condition number. The method P0 and the compatible case has similar condition numbers, but surprisingly the method P1 had condition numbers about ten times smaller, which

leads to the less than half number of iterations. This property is unaffected by σ, ρ or δ_2.

6. Conclusions. We have presented two new methods for the mixed-hybrid discretization of couplings between dimensions. Both methods were tested on a simple 2d-1d problem that provides an analytical solution. The experimentally determined orders of convergence are almost same for both methods, but the absolute errors are smaller for the method P1. This method also results into linear systems with better condition numbers and is more robust. The main drawback of both methods is worse resolution of the velocity near the fractures compared to the compatible discretization. This is natural since we use continuous approximation of the velocity over the fractures where the exact velocity field has a jump. To get better velocity field near the fractures one should enrich the discrete space with base functions that have unit jump over the fracture.

Unfortunately, nothing is known about theoretical properties of the proposed methods. The theory for approximation of mixed problems due to Brezzi and Fortin [2] is not directly applicable. This is obviously an important open question and space for further research.

REFERENCES

[1] Jan Březina and Milan Hokr. Mixed-Hybrid formulation of multidimensional fracture flow. In *Numerical Methods and Applications*, LNCS, Borovets, Bulgaria, 2010. Springer.

[2] M. Fortin and F. Brezzi. *Mixed and Hybrid Finite Element Methods*. Springer-Verlag Berlin and Heidelberg GmbH & Co. K, December 1991.

[3] H. H. Gerke and M. T. van Genuchten. Evaluation of a First-Order water transfer term for variably saturated Dual-Porosity flow models. *Water Resources Research*, 29(4):PP. 1225–1238.

[4] Vincent Martin, Jérôme Jaffré, and Jean E. Roberts. Modeling fractures and barriers as interfaces for flow in porous media. *SIAM Journal on Scientific Computing*, 26(5):1667, 2005.

[5] Volker Reichenberger, Hartmut Jakobs, Peter Bastian, and Rainer Helmig. A mixed-dimensional finite volume method for two-phase flow in fractured porous media. *Advances in Water Resources*, 29(7):1020–1036, July 2006.

[6] Jan Šembera, Jiří Maryška, Jiřina Královcová, and Otto Severýn. A novel approach to modelling of flow in fractured porous medium. *Kybernetika*, 43(4):577–588, 2007.

[7] J. Maryška, M. Rozložník, and M. Tůma. Mixed-hybrid finite element approximation of the potential fluid flow problem. *J. Comp. Appl. Math.*, 63:383–392, 1995.

[8] Martin Vohralik. A posteriori error estimates for Lowest-Order mixed finite element discretizations of Convection-Diffusion-Reaction equations. *SIAM Journal on Numerical Analysis*, 45(4):1570, 2007.

[9] Mary F. Wheeler, Tim Wildey, and Guangri Xue. Efficient algorithms for multiscale modeling in porous media. *Numerical Linear Algebra with Applications*, 17(5):771–785, September 2010.